Molten salt as heat transfer fluid for a 500 m^2 dish concentrator

Nicolás del Pozo[1], Rebecca Dunn[2] and John Pye[3]

[1] Research School of Engineering (RSE), Australian National University (ANU), Canberra ACT 0200, Australia.

Phone +61 2 6125 8778. ndelpozo@gmail.com

[2]RSE, ANU, Phone +61 2 6125 3072. rebecca.dunn@anu.edu.au [3]RSE, ANU, john.pye@anu.edu.au.

Abstract

A study into the integration of a molten salt based thermal storage system with the ANU SG4 500 m^2 dish solar concentrator was performed. Specifically, the objective was to research the behaviour of molten salt as a heat transfer fluid for the SG4 dish solar concentrator, including its receiver, auxiliary piping and accessories. A numerical model was developed to analyse the heat transfer at the receiver and also to obtain the hydraulic pressure losses and demand curve for the entire system. This case study was restricted to a receiver position of 90º, or facing downwards, as this position requires the highest molten salt flow, and hence gives a maximum sizing for system components.

The results indicate that the molten salt temperature profile inside the receiver is dominated by the solar irradiance profile over the cavity surface; with the heat exchange by radiation, conduction and natural convection having a lesser effect. Existing pipework, receiver tubes and rotary joints from the SG4 dish would need to be resized for reduced pressure drops. However, this initial investigation suggests that the use of molten salt as a heat transfer fluid for the ANU 500 m^2 dish is feasible, and warrants further investigation.

1. Introduction

The ANU 489 m^2 paraboloidal dish solar concentrator, or SG4 dish pictured in Figure 1, was completed in 2009. It has a 13.4 m focal length, altitude-azimuth tracking, and comprises 380 spherical glass-on-metal laminate mirror panels, as described by Lovegrove et al [1]. One of its key elements is the mono-tube boiler for direct steam generation (Figure 1) that receives the concentrated irradiance from the mirrors and transfers its energy to the passing flow of water that boils into high pressure steam.

Fig.1. The ANU SG4 dish (left), its current receiver (center) and the model geometry (right).

Energy storage systems provide solar thermal applications independence from solar radiation availability, allowing them to produce dispatchable power [2], [3], [4]. The aim of this project was to explore the use of MS as a heat transfer fluid (HTF) in the SG4 receiver. The physical properties of molten salt (MS) compared to water suggest marked differences in the heat flux transfer that can be achieved for a given receiver design. To achieve this, a numerical model of the steady-state heat transfer in the current SG4 receiver has been developed. This allows the estimation of the receiver and MS temperature profiles, physical properties and total dynamic head (TDH) under different flow scenarios.

2. Model

2.1 Fluid circuit for the SG4 Big Dish

In the current SG4 receiver, shown in Figure 1, the internal helical steel tube section comprises 16 mm OD x 12 mm ID mild steel tube in the lower part and a ¾" schedule 40 stainless steel pipe for the upper part. High-pressure steam exits from the top of the receiver and flows down through the steam line. The feed-water line consists of nearly 90 m of 5/8" ID and 1.6 mm thick steel pipe. The steam line is made of steel pipe and is approximately 95 m long, 1" ID and 3.2 mm thick. It is used to transport the superheated steam from the receiver back to the engine room.

One important design characteristic of the fluid circuit is the use of rotary joints to convey the feedwater and steam to and from the receiver, respectively, as two-axis tracking eliminates the possibility of fixed pipework.

2.2 Model receiver geometry

To estimate the steady-state heat transfer and MS properties, a model of the receiver with simpler geometry has been proposed. It consists of a 1.248 m long cylinder with a diameter of 0.68 m, vertically oriented. A disc of equal diameter closes the top aperture, while the bottom aperture is left open. The bottom 'hat-rim' section of the existing steam receiver is not considered in the present modelling.

Additionally, the cylinder has been divided into 48 segments along its axis, each of 26 mm height. Each segment represents a complete turn of the stainless steel helical tube through which MS flows. For conductive and convective heat transfer calculations, these elements were considered to have a tubular section. For radiative heat transfer, the elements were considered as flat rings. The disc on top was treated as a separate surface, while the aperture in the bottom, as a virtual surface. Thus a total of 50 independent surfaces were considered as shown in Figure 1.

A downward orientation of the receiver represents the lowest natural convection loss scenario [5]. Combined with the fact that peak direct normal irradiance generally occurs at solar noon, this scenario gives the maximum MS flow rate that the system will need to experience. Therefore, the downward-facing case was chosen as it presents a limiting case for the design of the balance of system, when frictional and thermal losses can be expected to be maximal. Clearly, annual performance modelling and thermo-economic assessment of this concept will require a more detailed heat loss model incorporating thermal losses as a function of collector zenith angle, but that modelling has not been undertaken in this study.

2.3 Heat transfer at the receiver

To study the behaviour of MS as a HTF for the system, it was necessary to estimate its physical properties. As these vary with temperature, the present model evaluates MS properties through the receiver, and takes them into consideration in calculation of the internal heat transfer and pressure drop for each tube segment. Beyond the receiver, the MS flow was considered adiabatic due to pipework insulation, so its physical properties were assumed equal to the cold tank temperature upstream and to the receiver outlet temperature downstream.

2.3.1. Absorbed Irradiance

An irradiance flux profile developed by Zapata et al [6] with the aid of OPTICAD 10.0 ray-tracing software was utilized to quantify the irradiance over segments 1-48, each of $0.083\ m^2$ area. This profile not only considered the direct radiation from the field but also the effect of multiple reflections inside the cavity. The cavity interior has an absorptivity of 89% and reflectivity of 11% [7], so that after three reflections, only 0.13% of the incident radiation was left unabsorbed. Therefore, the cavity as a whole may be assumed as a black body for practical purposes. The total considered irradiance over the cavity inner vertical surfaces is 397.81 kW. The irradiance along the inner surface of the cavity is presented in Figure 2.

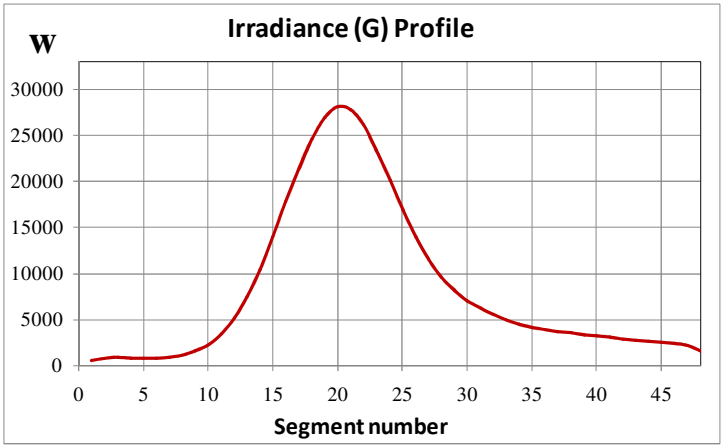

Fig. 2. Irradiance for each tube segment, numbered vertically upwards from receiver opening.

2.3.2. Natural convection

The experimentally-validated correlation found by Taumoefolau [8] for natural convective thermal losses of a similar cavity was considered. This correlation, in a similar form to the Stine correlation, allows natural convection results to be obtained for the case where the cavity is facing downward, as in the studied case. The subscript *l* represents the characteristic length, which in this case is the diameter of the cavity.

$$Nu_l = 0.414Ra^{0.25}\left(\frac{A_a}{A_c}\right)^S h(\bar{\theta}), \text{ where } S = 2.2834 - 2.686\left(\frac{A_a}{A_c}\right)^{0.1}$$

$h(\theta)$ is a dimensionless function of the inclination of the cavity. For an inclination angle larger than the angle of maximum convection loss, as in this case, this function is:

$$h(\overline{\theta}) = \frac{1}{h_0}\left(1 - cos\left[\overline{\theta}^{1.2}\pi\right]\right) + 0.08$$

where $h_0 = 1 - cos\left(\overline{\theta}(\theta = 0)^{1.2}\pi\right)$,

$$\overline{\theta} = \frac{\theta - 90°}{\theta_{max} - 90°}$$

$$\theta_{max} = -6° - 318°\left(\frac{A_a}{A_c}\right)$$

From the geometry described, the inclination angle for the study case is 90° and the ratio of areas is A_a/A_c =0.107. Hence, we obtain $\theta_{max} = -40.04°$, $h(\overline{\theta}) = 0.08$ and s= 0.135. Then, using the average wall temperature, an ambient temperature of 300 K and air properties at film temperature, the global Nusselt number and the global heat transfer coefficient for the entire cavity was obtained. Finally, using Newton's law of cooling, the global heat loss from the cavity was directly estimated.

Although the correlation is in numerical agreement with the measured data by Taumoefolau [8], the stagnation of the air inside the cavity suggests the dominant mechanism of heat transfer in this case is conduction rather than natural convection. In any case, this mechanism had a minor effect on the heat losses, accounting for only 379 W (6.9 %) of total heat losses under the medium flow rate scenario (see Section 2.4 below for definition of medium flow rate).

2.3.3 Conductive heat losses

Conductive losses were calculated for the receiver external walls. Full details are given by del Pozo [9]. The vertical wall of the cavity was divided into 48 annular segments, each corresponding to a helical tube segment.

The insulation, Rockwool 650, has a thermal conductivity coefficient (in W/m/K) that varies with temperature (in Kelvin) according to $k = 0.031e^{0.326T}$. One-dimensional conduction was assumed. Knowing that the heat flow conducted from the interior of the cavity to the ambient has to be equal to that rejected from the wall to the ambient, the wall temperature was obtained by iteration for each annular segment. The

properties of the air film dependent of the temperature were also adjusted in this process since they depend on the wall temperature.

For the top disc that closes the receiver (50th surface), the procedure was similar, assuming an internal temperature equal to the uppermost helical tube segment. Conduction losses represented 14.54% of the total heat losses (799 W) under the medium flow rate scenario (see Section 2.4 below).

2.3.4. Radiative heat losses

The surface temperature profile of the 48 segments also included radiative heat losses and exchange among the internal surfaces of the cavity. The virtual surface at the bottom was assumed at ambient temperature (20°C), and the top disc at the same temperature of the uppermost tube segment.

To estimate the view factors, three different relations were utilized. The relation for a tubular segment with respect to other tubular segments was estimated from Buschman and Pittman [10]. Similarly, the view factor from an arbitrary segment to the top and bottom disc-shaped surfaces was estimated from Buraczewski and Stasiek [11]. Finally, for the view factor between the top and bottom surfaces, a relation presented by Howell et al [12] was utilized. The emissivity was taken as 0.89 for all surfaces as was proposed by Bannister [7].

Afterwards, the resulting radiative heat losses were accounted to re-calculate the tube surface and MS temperatures following an iterative process until the surface temperatures converged.

2.3.5. Heat Transfer to the Molten Salt

The model assumes steady-state regime. Hence, the energy balance demands that all the absorbed irradiance, minus losses, is transferred to the MS. The internal energy of the MS flow was estimated in terms of its isobaric heat capacity that is, in turn, dependent on its temperature. Therefore, by using the cold tank temperature (288 °C) as a boundary condition, the temperature of the MS inside each of the 48 segments was obtained as a partial result of the iterative calculation process described earlier.

$$T_{i,ms} = \frac{\varepsilon G_i - losses}{\left(C_{p_{i-1}}.\dot{m}\right)} + T_{i-1,ms}$$

The average outer surface temperature of each tube segment was estimated as follows:

$$T_{i,sur} = (\varepsilon G_i - losses) \cdot (1/(h_i \cdot A_i) + R_{th,tube}) + T_{i,ms}$$

As a consequence, a set of tube surface temperatures that satisfy radiative, natural convective and conductive heat losses was obtained. Perhaps more important is the MS temperature profile inside the receiver tubes that allows to estimate its physical properties and the mass flow corresponding to any given outlet temperature.

2.4 Hydraulic calculations

Following the heat transfer calculation procedure outlined in Section 2.3, the MS mass flow was adjusted to meet three different maximum temperatures at the outlet of the receiver.

The first is given by the minimum mass flow to achieve the highest allowable MS temperature (600ºC) within the thermal stability interval of the properties published by Zavoico [13]. This mass flow corresponds to 0.827 $\mathrm{kg/s}$.

The second scenario meets the temperature of the hot tank (565 ℃) at the Solar Two project as was described by Reilly and Kolb [2]. The MS mass flow to achieve this is 0.934 $\mathrm{kg/s}$.

The third scenario corresponds to 1.273 $\mathrm{kg/s}$ since that mass flow allows to achieve a maximum velocity of 2.28 $\mathrm{m/s}$, as was recommended by Nejedlý and Matal [14] for MS flows inside a certain cooling system. Although higher flow velocities are achievable, this value is high enough to illustrate the issues that may arise from high flows. This flow yields a maximum temperature of 492ºC, still well within the practical applicability range of MS, and still providing a high inlet temperature for the steam cycle.

With these mass flow scenarios, it was possible to estimate the pressure drop and pump requirements across the complete MS circuit. In order to estimate the frictional head losses for the flow, a friction factor has to be utilized. According to VDI-GVC [15], for a helical tube, this is:

$$f = \frac{0.3164}{Re^{0.25}}\left[1 + 0.095\left(\frac{D_{tube,in}}{D_{winding}}\right)^{0.5} Re^{0.25}\right]$$

As expected, this estimation predicts slightly higher frictional loses than the Swamee and Jain [16] equation developed for straight pipes. If we refer to the Darcy-Weisbach equation for head loss, it is easy to realize the friction factor and pressure gradient vary along the helical tube of the receiver as the physical properties and velocity of the MS change. Applying the Darcy-Weisbach equation to every segment of the flow inside the tube, the overall head loss of the receiver was obtained by simple addition:

$$\Delta H_{receiver} = \sum_{i=1}^{48} \frac{f_i L_i}{D} \frac{U_i^2}{2g}$$

For the rest of the system, the MS flow was considered adiabatic. The boundaries of the hydraulic model are the tie-in points of the pump and the hot tank entrance, leaving the entire steam generation and heat exchange circuit and power block out of the scope.

The elements of the current fluid transport system were identified on site and their singular head loss coefficients, extracted from Crane Valve Co. documentation [17]. For the case of the rotary joints, the estimation of an equivalent minor loss coefficient (K) was done equating Siangsukone [18] least squares fit on experimental data for pressure drop of water, and corrected by the density ratio between water and MS, with the minor loss equation. Hence:

$$K = \frac{(3316.6\dot{m}^2 + 45.32\dot{m} + 1.4877) \cdot 1000/(\rho g)\left[\frac{\rho_{water}}{\rho_{molten\ salt}}\right]}{U^2/2g}$$

where the velocity corresponds to that of the MS flow. For mass flows in the range of 0.6-1.5 kg/s this yields unacceptable pressure drops (1-7 MPa) and an equivalent K average value of 209 for the flow range of interest. This value is significantly high and points out the necessity of redesigning the rotary joints for high flows. The flow is considerably higher than when using water/steam in the SG4 dish due to the higher enthalpy of vaporization of water compared to the relatively modest heat capacity of MS. In order to avoid distorting the rest of the results, a value of 8.2 was adopted instead for further calculations as this allowed a clearer understanding of the performance of the remaining elements of the system.

3. Results

3.1 Temperature Profiles

Figure 3 shows the surface and MS temperature profiles in addition to the net heat losses at each segment under the medium MS mass flow scenario (0.934 kg/s).

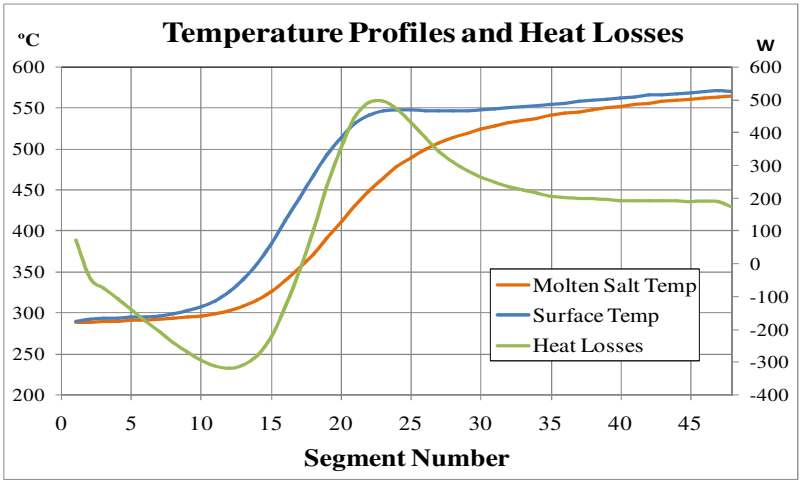

Fig. 3. Temperature Profiles and Heat Losses.

The MS temperature profile exhibits similar behaviour to the surface temperature profile, as the two are intrinsically linked. Heat exchange is largely dominated by the radiative mechanism. While negative values for heat loss observed toward the aperture denote a net positive gain of heat due to re-radiation, positive values indicate losses. These are very significant around the middle of the cavity length-wise, due to the high surface temperature.

3.2 Heat transfer coefficient

Figure 4 shows the development of kinematic viscosity and the heat transfer coefficient along the helical tube for the maximum flow rate scenario (1.273 kg/s).

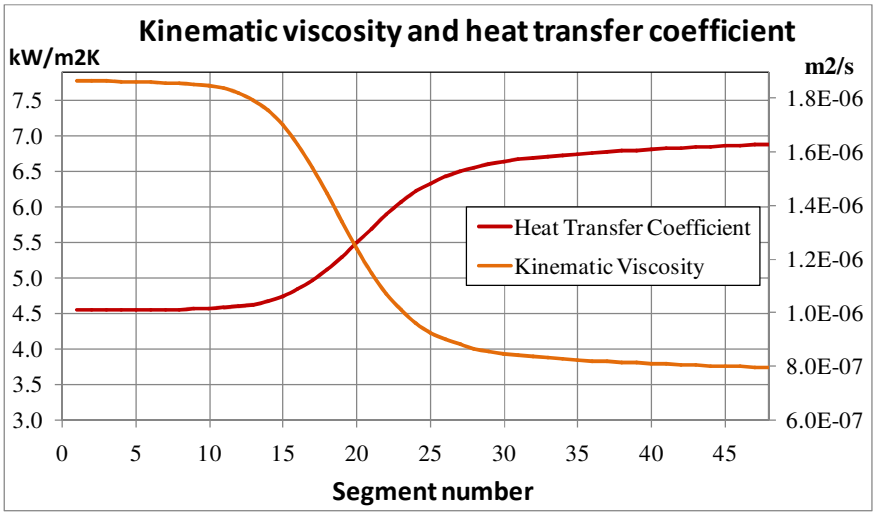

Fig. 4. Molten salt kinematic viscosity and heat transfer coefficient.

The heat transfer coefficient from the tube inner surface to the MS is highly dependent on the kinematic viscosity of the MS. This property changes as the temperature of the MS changes along its path. This result suggests that a receiver designed so as to allow significant preheating of the MS will achieve a higher overall heat transfer coefficient.

3.3 Dynamic head

A model of pressure drops through the balance of system was established, initially based on the assumption of no modifications to the existing pipework. Figure 5 summarizes the head losses across main elements that contribute to the system total dynamic head (TDH) at different MS mass flows. Note that in this case, the rotary joints have been considered with a minor loss coefficient (K) of 8.2.

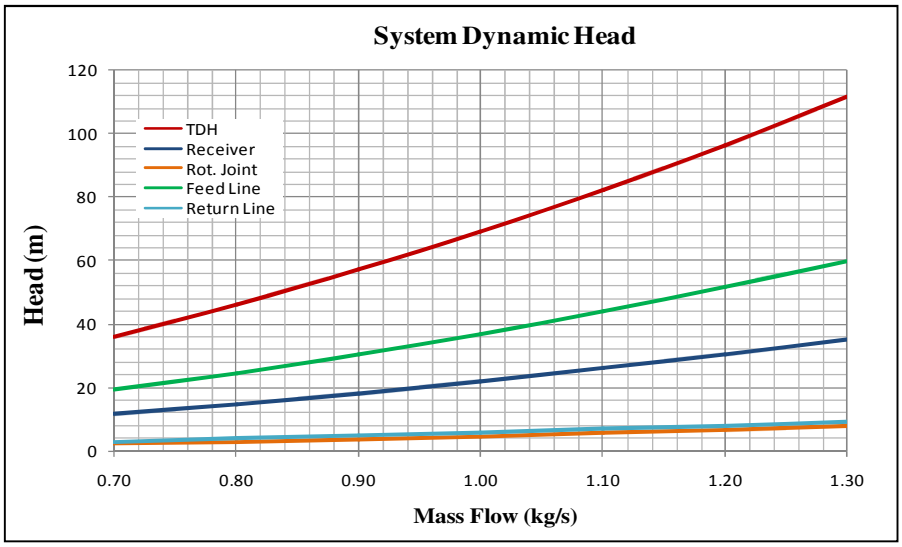

Fig. 5. System dynamic head.

The high heads observed suggest the use of a multi-staged vertical pump at the cold tank. However, because of the very modest flow that would be handled by an individual SG4 dish, commercial pumps are virtually unavailable. Additionally, the cost and complexity of the whole SG4 system suggest that an array of dishes with a central storage, pump, control and auxiliary systems can be much more cost efficient due the inherent synergies.

In the case of the receiver, at the lowest mass flow rate scenario proposed, the frictional head losses were 34.1 m. This suggests that an increase in the internal diameter of its helical tube needs to be made. The piping accessories, fittings and bends showed moderate head losses throughout the range of flow rate with the exception of the original rotary joints, for which its minor head loss coefficient is significantly higher than the rest of the accessories (K=209). This highlights the necessity of reviewing its design to achieve a moderate value.

The feed and return pipelines showed the need for a minimum pipe diameter. While the return line yielded a frictional head loss of only 7 m, over 90 m long, the feed line accounted for over 50 m head loss over 95 meters, both under the maximum flow scenario. This represents the highest pressure drop and pumping power consumption. The main reason behind this is the required flow would be considerably higher than when using water/steam, as in the original SG4 design due the higher enthalpy of vaporization of water compared to the relatively modest heat capacity of MS. However, the net result is a substantial increase in velocity and head losses. This result suggests a change in the diameter of the feed line, for example to that of the return pipeline, to moderate its frictional losses.

The hydraulic power required for pumping under the three scenarios was estimated with a pump efficiency of 100% in lieu of reliable data from any manufacturer because of the very low flow rates. The pump powers thus consumed were 1339 W, 561 W and 399 W for the high, medium and low flow scenarios respectively.

4. Conclusion

This preliminary model suggests that the use of molten salt in solar paraboloidal dish concentrators is feasible, and open to further investigation. Existing pipework, receiver tubes and rotary joints from the SG4 dish would need to be resized for reduced pressure drops.

Future work could investigate the effect that transient phenomena, equivalent to water-hammer, can have on the internal pressure of the piping when using molten salt. Additionally, HAZOP and a Failure Modes and Effects Analysis to the proposed system could be developed to ensure its safety. This paper has not considered issues associated with heat tracing and blockage, and these issues still require investigation.

Acknowledgements

The authors wish to acknowledge the assistance of the Solar Thermal Group at the Australian National University in the preparation of this paper, in particular that of Mr Greg Burgess and Mr José Zapata.

References

[1] Lovegrove K., Burgess G., Pye J. (2011). "A new 500 m^2 paraboloidal dish solar concentrator." Solar Energy, 85(4), pp. 620-626.

[2] Reilly H. and Kolb G. (2001). "An Evaluation of Molten-Salt Power Towers including results of the Solar Two Project." Solar Thermal Technology Department, Sandia National Laboratories, NM, Tech. Report SAND2001-3674.

[3] S. Relloso and E. Delgado (2009), "Experience with molten salt thermal storage in a commercial parabolic trough plant. Andasol-1 commissioning and operation," in Proceedings of the 15th SolarPACES Conference, Berlin.

[4] J. I. Burgaleta, S. Arias and I. B. Salbidegoitia (2009), "Operative advantages of a central tower solar plant with thermal storage system," in Proceedings of the 15th SolarPACES Conference, Berlin.

[5] Paitoonsurikarn S. (2006), "Study of a Dissociation Reactor for an Ammonia-Based Solar Thermal System". PhD Thesis, Department of Engineering, Australian National University, Canberra, Australia.

[6] Zapata J., Lovegrove K. and Pye J. (2010). "Steam receiver Models for Solar Dish Concentrators: Two Models Compared," in Proceedings of the 16th SolarPACES Conference, Perpignan, 2010.

[7] Bannister P. (1991). "An Experimental and Analytical Assessment of a Steam Rankine Solar Thermal System." Ph.D. Thesis, The Australian National University, Research School of Physical Sciences and Engineering Canberra, Australia.

[8] Taumoefolau T. (2004). "Experimental Investigation of Convection Loss from a Model Solar Concentrator Cavity Receiver," Master of Philosophy Thesis, Department of Engineering, Australian National University, Canberra, Australia.

[9] Del Pozo N. (2011). "Molten salt as heat transfer fluid for a 500 m^2 dish concentrator," Master of Engineering Thesis, Department of Engineering, Australian National University, Canberra, Australia.

[10] Buschman A. and Pittman C.(1961). "Configuration factors for exchange of radiant energy between axisymmetrical sections of cylinders, cones, and hemispheres and their bases," NASA TN D-944, USA.

[11] Buraczewski C. and Stasiek J. (1983). "Application of generalized Pythagoras theorem to calculation of configuration factors between surfaces of channels of revolution." International Journal of Heat & Fluid Flow, vol. 4, no. 3, pp. 157-160.

[12] Howell J., Siegel R. and Menguc M. (2010). *Thermal Radiation Heat Transfer*, 5th ed., Taylor and Francis/CRC, New York, USA.

[13] Zavoico A. (2001). "Solar Power Tower Design Basis Document". Revision 0, SAND2001-2100. Sandia National Laboratories, printed July 2001.

[14] Nejedlý M. and Matal O. (2003). "Studies on Components for a Molten Salt Reactor". Brno University of Technology, Institute of Power Engineering, Czech Republic.

[15] *VDI-Gesellschaft Verfahrenstechnik und Chemieingenieurwesen (GVC)* (2006). Wärmeatlas. ISBN 978-3-540-25504-8, Springer-Verlag, Berlin.

[16] Swamee P., and Jain A. (1976). "Explicit Equations for Pipe Flow Problems." Journal of the Hydraulics Division,Vol. 102, No. 5, pp. 657-664.

[17] Crane Valve Co. (1998). *Flow of Fluids Through Valves, Fittings & Pipe TP-410*. New York, USA.

[18] Siangsukone P. (2005, p.178). "Transient Simulation and Modelling of a Dish Solar Thermal Power System". PhD Thesis, Department of Engineering, Australian National University, Canberra, Australia.